

# On the origin of the gamma-ray emission toward SNR CTB 37A with Fermi-LAT

S. Abdollahi<sup>1</sup>, J. Ballet<sup>2</sup>, T. Mizuno<sup>1</sup>, Y. Fukazawa<sup>1</sup>, H. Katagiri<sup>3</sup>  
On behalf of the Fermi Large Area Telescope Collaboration

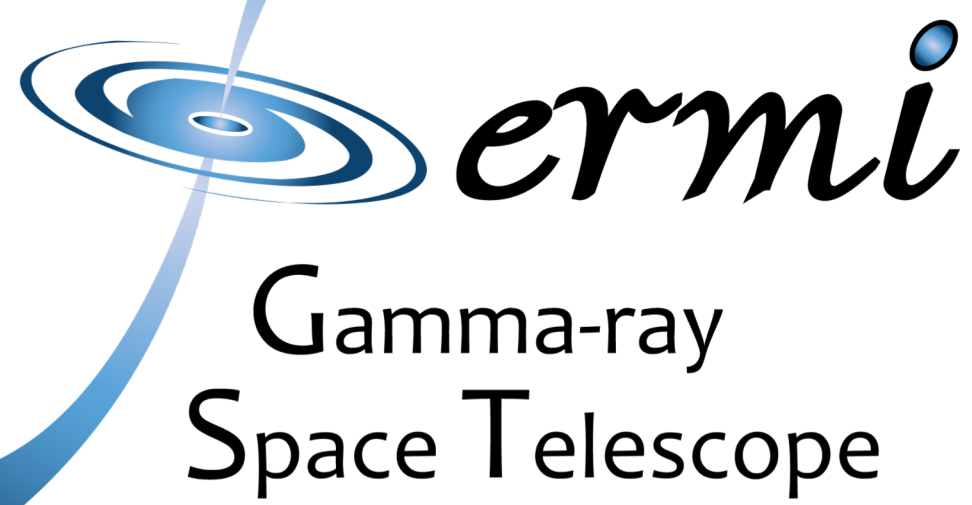
<sup>1</sup>Department of Physical Sciences, Hiroshima University, Higashi-Hiroshima, Hiroshima 739-8526, Japan

<sup>2</sup>Laboratoire AIM, CEA-IRFU/CNRS/Université Paris Diderot, Service d'Astrophysique, CEA Saclay, 91191 Gif sur Yvette, France

<sup>3</sup>College of Science, Ibaraki University, 2-1-1, Bunkyo, Mito 310-8512, Japan



HIROSHIMA UNIVERSITY



**Abstract** “Supernova remnants (SNRs) are believed to be one of the major sources of Galactic cosmic rays (CRs) up to  $\sim 10^{15}$  eV. Middle-aged SNR CTB 37A, located in a very complex region, is known to interact with several adjacent dense molecular clouds through detection of shocked  $H_2$  and OH 1720 MHz maser emission. The TeV  $\gamma$ -ray source HESS J1714–385 and the X-ray source CXOU J171419.8–383023 are both offset to the west from the geometric center of the remnant and are embedded within the extended radio shell, though it is still not clear whether the TeV  $\gamma$ -ray emission originates in the SNR or in a plausible pulsar wind nebula (PWN). In the present work, we use eight years of Fermi-LAT Pass 8 data to perform detailed morphological and spectral studies of the  $\gamma$ -ray emission. Based on the spatial and spectral characteristics of the SNR, we discuss the possibility of a composite nature for CTB 37A to explain the broadband spectrum and to constrain the physical parameters of the SNR, which helps us to elucidate the nature of the  $\gamma$ -ray emission toward the CTB 37A system.”

## Morphological Analysis

Because of a particularly crowded region around the remnant which can affect the results, we iteratively fitted the position and extension of CTB 37A and the position of two nearby sources (CTB 37B and FL8Y J1714.8-3850, both at  $< 0.5^\circ$  from the region of interest center) until it converges and the fit parameters are stable. Comparison of three different spatial models used to measure the remnant extension favors a Gaussian over a uniform disk and a point source hypothesis with  $TS_{\text{ext}} = 33.10$  and  $r_{68} = (0.116 \pm 0.014_{\text{stat}} \pm 0.017_{\text{sys}})^\circ$  (corresponding to the 68% containment radius) at above 1 GeV.

Table 1. (Top) Results of spatial analysis using “pointlike” with all data in the 1-200 GeV energy range assuming a LogParabola (LP) for CTB 37A and FL8Y source and a Power-Law for CTB 37B. (Bottom) Fitted spatial and spectral parameters of CTB 37A modeled by a Gaussian template and its two nearby sources. The FL8Y source is not bright but it has effect on the source extension and localization. For the disk,  $r_{68,\text{disk}} = 0.82 \sigma$  and for the Gaussian model,  $r_{68,\text{Gaussian}} = 1.51 \sigma$ .

Spatial Model	$r_{68}$ ( $^\circ$ ) $\pm$ stat. $\pm$ sys.	$TS_{\text{ext}}$	$N_{\text{dof}}$
Disk	$0.142 \pm 0.025 \pm 0.022$	19.61	6
Gaussian	$0.116 \pm 0.014 \pm 0.017$	33.10	6

Source name	R.A. ( $^\circ$ )	Dec. ( $^\circ$ )	$r_{68}$ ( $^\circ$ )	TS	Spectral index ( $\alpha$ )	Curvature ( $\beta$ )
CTB 37A	$258.625 \pm 0.007$	$-38.513 \pm 0.008$	$0.116 \pm 0.014$	1298	$2.086 \pm 0.135$	$0.103 \pm 0.043$
FL8Y J1714.8-3850	$258.777 \pm 0.026$	$-38.761 \pm 0.018$	---	128	$2.661 \pm 0.214$	$0.351 \pm 0.245$
CTB 37B	$258.533 \pm 0.017$	$-38.185 \pm 0.014$	---	82	$1.611 \pm 0.127$	---

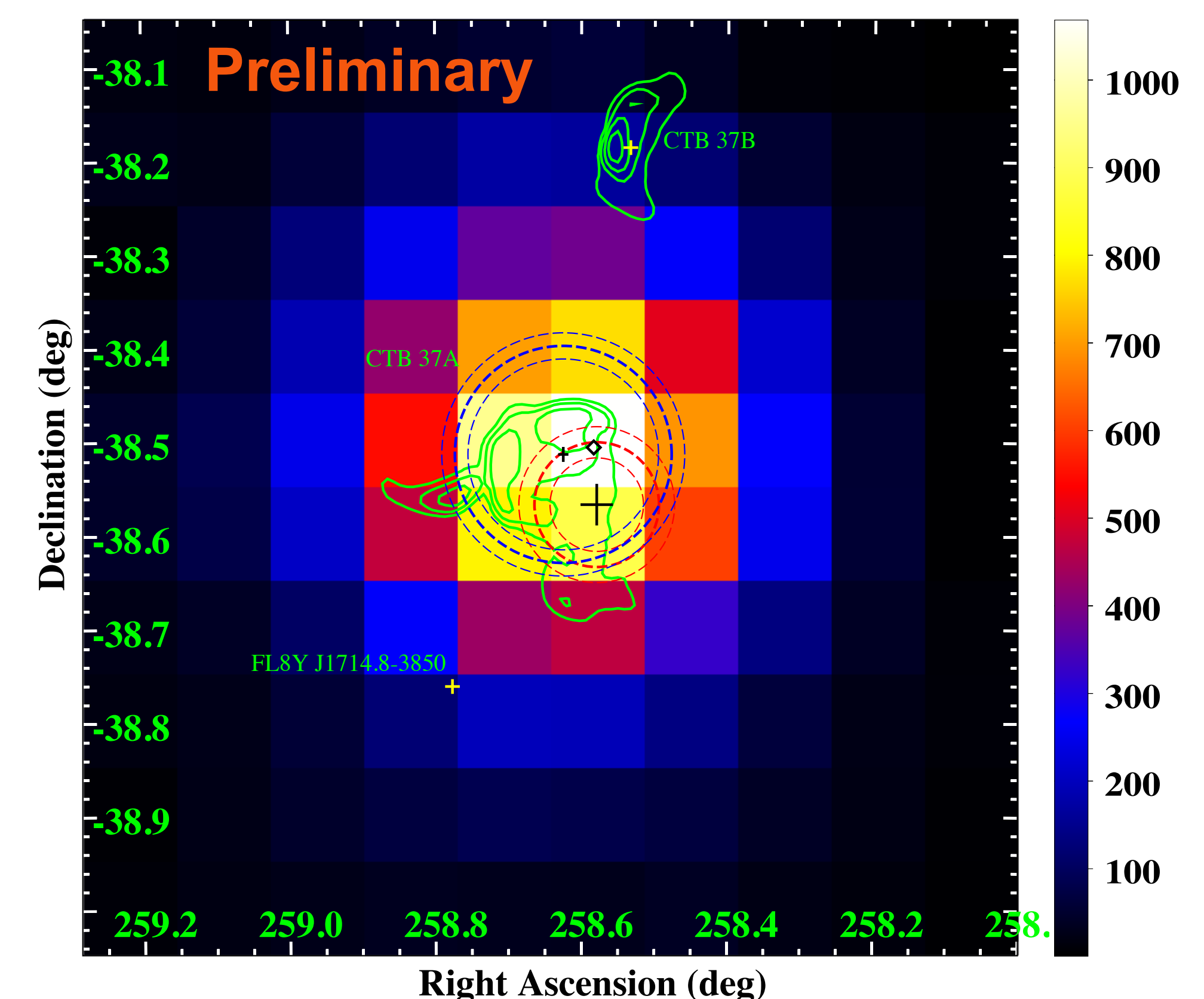


Figure 1. Test Statistic map in 1-200 GeV energy range. The black crosses indicate the position of CTB 37A and HESS J1714.5-385 and their statistical errors. The black diamond corresponds to the position of the X-ray source CXOU J171419.8-383023. Yellow crosses indicate the position of FL8Y J1714.8-3850 and CTB 37B. The 68% containment radii obtained by the Gaussian model for CTB 37A and the HESS source [1] are shown with thick dashed blue and red circles, respectively. The inner and outer circles represent the statistical errors on the extension.

## Spectral Analysis

Spectral analysis was performed between 0.2 GeV and 200 GeV using an optimized data set in order to minimize low-energy systematic effects. The energy spectrum becomes softer above 10 GeV than the TeV spectrum which strengthens the idea of different origins for the GeV and TeV emissions. From the global fit using a LP (see below table), a photon flux  $(5.47 \pm 2.06) \times 10^{-8}$  ph  $\text{cm}^{-2} \text{s}^{-1}$  and an energy flux  $(5.36 \pm 1.02) \times 10^{-8}$  GeV  $\text{cm}^{-2} \text{s}^{-1}$  were obtained.

Method	CTB 37A spectral parameters		Note
	Spectral index at 1 GeV ( $\alpha$ )	Curvature ( $\beta$ )	
SummedLike	$1.844 \pm 0.192$	$0.215 \pm 0.063$	All data above 0.2 GeV
SummedLike	$1.924 \pm 0.192$	$0.184 \pm 0.049$	Optimized data selection

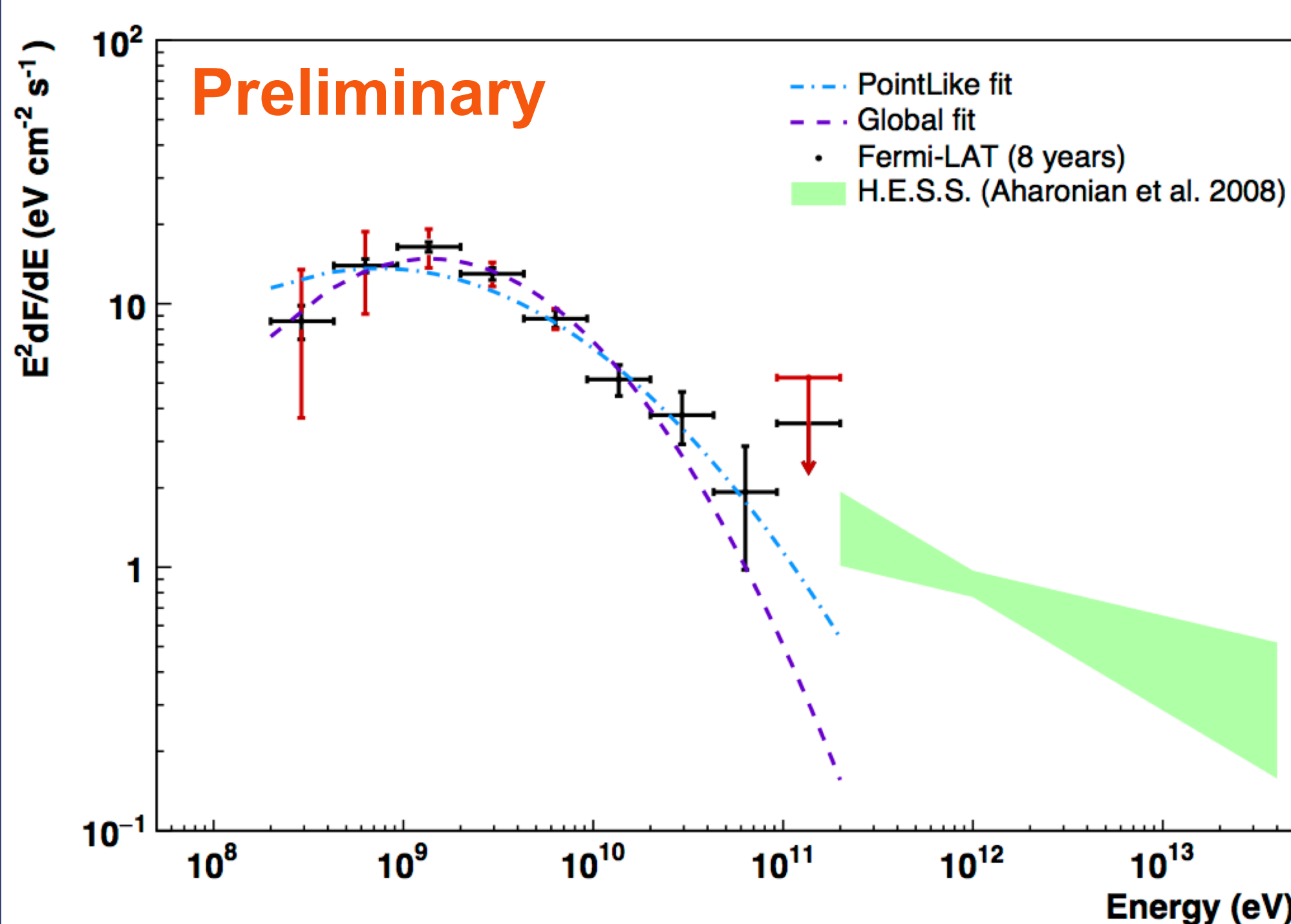


Figure 2. The vertical black and red error bars represent statistical and systematic errors, respectively. The blue curve shows the fit with pointlike above 1 GeV which is extrapolated down to 0.2 GeV for better comparison. The violet curve shows the global fit over the whole energy range (0.2-200 GeV) for the optimized data. Energy dispersion correction is taken into account.

## Spectral Modeling & Discussion

Assuming the Sedov stage of evolution and following Devin et al., 2018, we derived dynamical characteristics of the SNR and constrained the spectral characteristics using the multi-wavelength observations. Between the hadronic and leptonic emission models, the results demonstrate that the gamma-ray emission is more likely coming from the surrounding shocked molecular clouds. In this scenario, the GeV and radio data can be well explained if 0.75% of the kinetic energy released by the supernova is transferred to the radiative shock and the electron to proton ratio  $K_{ep} = 0.03$  is taken.

Scenario	B ( $\mu\text{G}$ )	$W_p$ ( $\times 10^{49}$ erg)	$K_{ep}$	$\Gamma_{e,1}/\Gamma_{e,2}$	$E_b$ (TeV)	$E_{\text{max},e}$ (TeV)	$\Gamma_p$	$E_{\text{max},p}$ (TeV)	$n_0$ ( $\text{cm}^{-3}$ )
Leptonic	20	5.7	1	1.66/2.66	1.66	1.66	2	1.66	0.64
<b>Hadronic</b>									
Main shock	10	5.7	0.03	2/3	0.83	0.83	2	0.83	0.64
Radiative shock	31.39								45.70
Cooled regions	518	0.43	0.03	1.66/2.66	0.02	0.03	2	0.03	3162.3

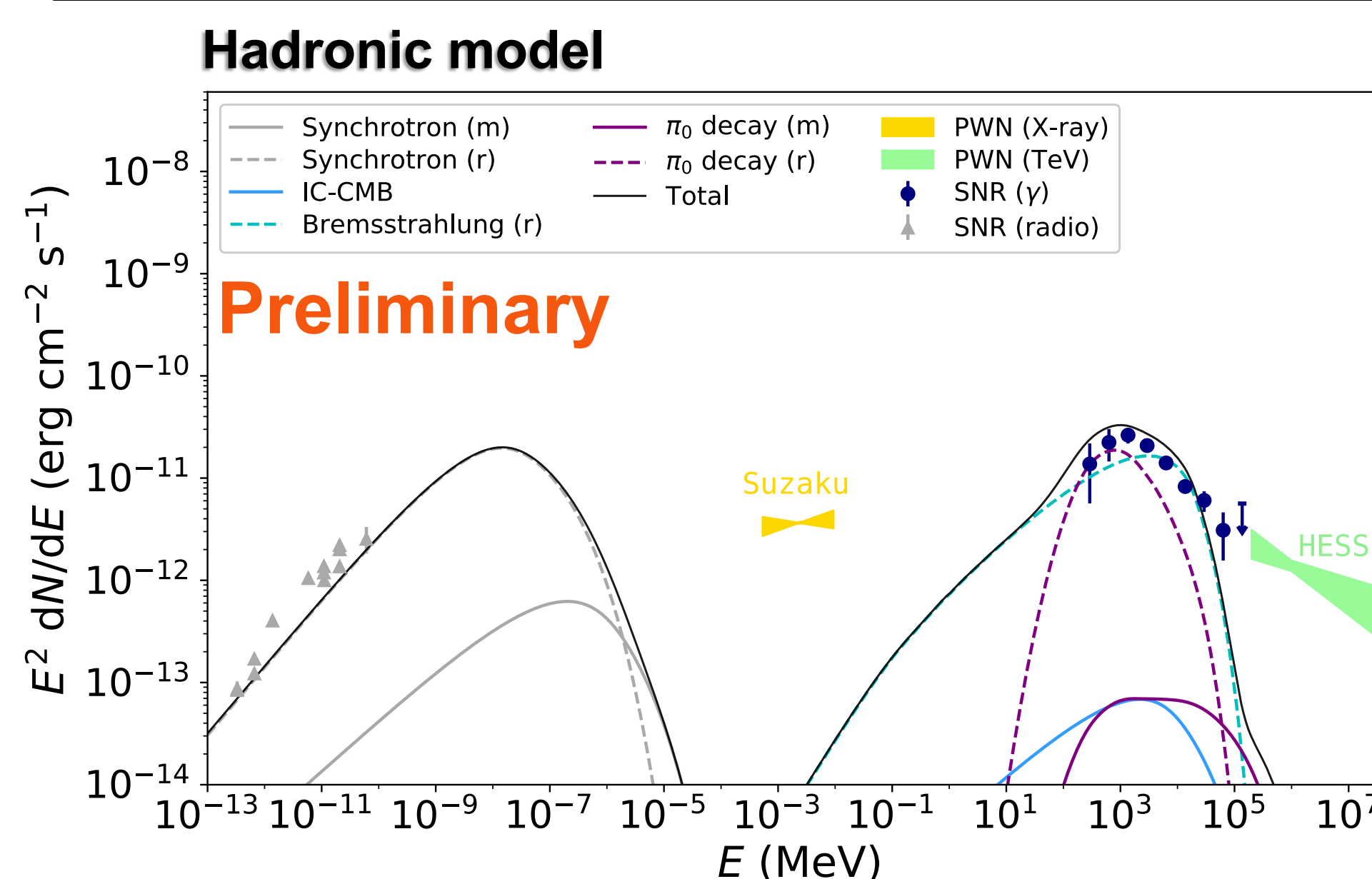


Figure 3. The broadband emission toward CTB 37A with the hadronic model based on the shocked clouds model with the parameters tabulated above. The density in the cooled regions is taken from the infrared observations, and the spectral index for the electrons in the radiative shock is from radio data.

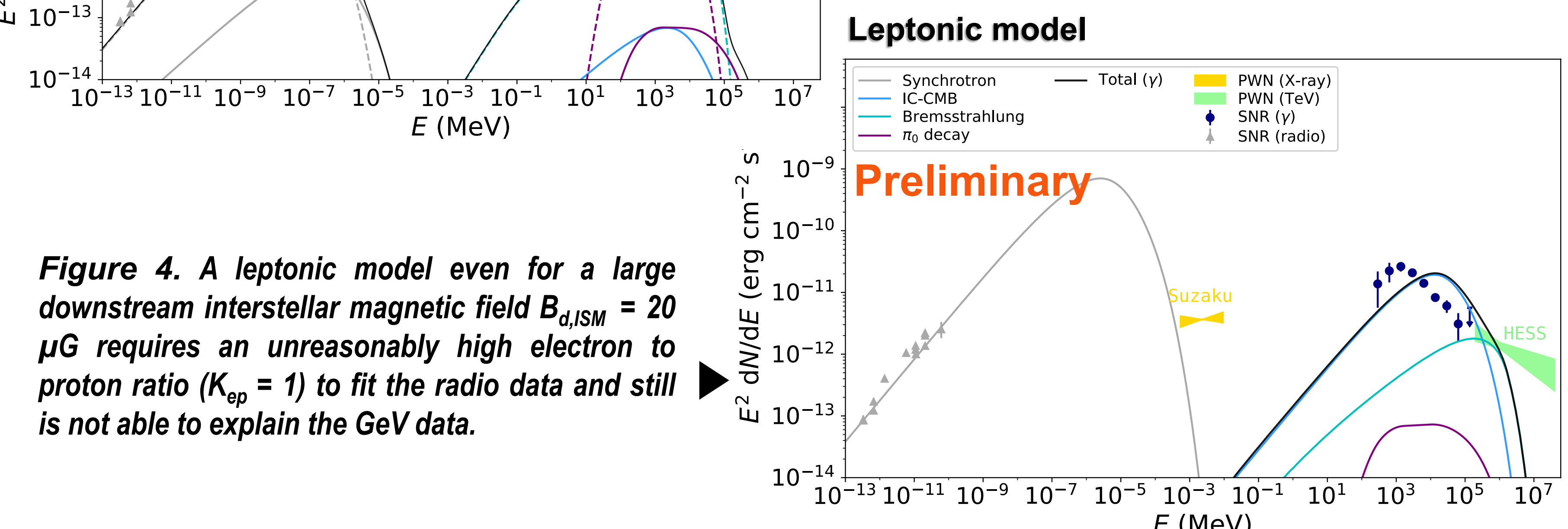


Figure 4. A leptonic model even for a large downstream interstellar magnetic field  $B_{d,ISM} = 20 \mu\text{G}$  requires an unreasonably high electron to proton ratio ( $K_{ep} = 1$ ) to fit the radio data and still is not able to explain the GeV data.

## References & info

- [1] Aharonian, F., et al. 2008, A&A, 490, 685-693
- [2] Pannuti, T. G., Rho, J., Heinke, C. O., & Moffitt, W. P. 2014, AJ, 147, 55
- [3] Whiteoak, J. B. Z., & Green, A. J. 1996, A&AS, 118, 329-380
- [4] Andersen, M., Rho, J., Reach, W. T., Hewitt, J. W., & Bernard, J. P. 2011, ApJ, 742, 7
- [5] Devin, J., Acero, F., Ballet, J., & Schmid, J. 2018, A&A, 617, A5
- [6] Uchiyama, Y., Blandford, R. D., Funk, S., Tajima, H., & Tanaka, T. 2010, ApJL, 723, L122